Mon. Not. R. Astron. Soc. **318**, 368–374 (2000)

Episodic absorption in the outflow of the old nova V603 Aquilae

Raman K. Prinja,[1]★ Christian Knigge,[2]† F. A. Ringwald[3]‡ and Richard A. Wade[4]

[1]*Department of Physics and Astronomy, University College London, Gower St, London WC1E 6BT*
[2]*Department of Astronomy, Columbia University, 555 West 120th Street, New York, NY 10027, USA*
[3]*Department of Physics and Space Sciences, Florida Institute of Technology, 150 West University Boulevard, Melbourne, FL 32901-6988, USA*
[4]*Department of Astronomy and Astrophysics, Pennsylvania State University, 525 Davey Laboratory, University Park, PA 16802-6305, USA*

Accepted 2000 May 12. Received 2000 April 19; in original form 2000 February 17

ABSTRACT

We report on the time-dependent behaviour of ultraviolet spectral lines in *Hubble Space Telescope* Goddard High-Resolution Spectrograph data of the classical nova V603 Aql. In particular, episodic blueshifted absorption (extending to $\sim -2500\,\mathrm{km\,s^{-1}}$) is present, with a variability time-scale down to ~1 min. The data provide a rare opportunity to study the rapid evolution of absorption structures that may be associated with accretion-disc winds in cataclysmic variables. At least three absorption events are recorded (at blueward velocities only) over ~5 h, each lasting ~10–15 min. The derived velocity, acceleration and optical depth properties provide an empirical picture of stochastically variable structures in the outflow, with no evidence for short-term (less than ~1 h) cyclic or modulated behaviour in the overall absorption properties. In contrast, the emission components of the ultraviolet resonance lines are very stable in velocity and strength in this low-inclination system. On at least two occasions there is an intriguing short-term 'flare' in the ultraviolet continuum flux (of up to ~40 per cent). Though there is no clear one-to-one relation in these data between the continuum fluctuations and the occurrence of the absorption events, the time-scales for the two variable phenomena are essentially the same. The irregular absorption episodes in the ultraviolet data of V603 Aql presently defy a clear physical interpretation. Their overall characteristics are discussed in the context of instabilities in radiation-pressure-driven disc winds.

Key words: stars: individual: V603 Aql – stars: mass-loss – novae, cataclysmic variables.

1 INTRODUCTION

This paper presents results from an ongoing programme to diagnose highly time-dependent outflows from cataclysmic variable (CV) binaries, based primarily on absorption-line profile signatures in rapid *Hubble Space Telescope* (*HST*) ultraviolet spectroscopy. Previously, we reported on the highly structured and erratic outflow from the nova-like system, BZ Cam, where substantial changes are present in wind-formed ultraviolet lines on time-scales down to ~100 s. (Prinja et al. 2000; hereafter PRWK). We follow that study here with fast ultraviolet spectroscopy of the classical nova V603 Aql, using data secured during the same *HST* programme in 1996 (Prog. ID 6661).

V603 Aql has received a lot of attention in the past owing to its substantial outburst in 1918 June (Nova Aquila 1918), during which it brightened by 13 mag to reach a visual magnitude of −1.1 [see, for example, summaries by Payne-Gaposchkin (1957) and Clark & Stephenson (1977)]. The ejected envelope from the fast nova was soon detected (Barnard 1919) and observed with a uniform expansion rate (Weaver 1974); the nebulosity is now rather dispersed and no longer discernible (e.g. Haefner & Metz 1985). The system is known to be a cataclysmic variable binary with an orbital period of 3 h 18.9 min (Drechsel, Rahe & Wargau 1982). This spectroscopically determined period is, however, ~5 per cent less than that derived from photometry (e.g. Patterson et al. 1993). This suggests a 'super-hump' origin for the photometric variability, i.e. the accretion disc in V603 Aql may be precessing as a result of gravitational perturbations owing to the secondary star. The small radial velocity variations ($\sim 30\,\mathrm{km\,s^{-1}}$) of the relatively narrow optical emission lines suggest that V603 Aql has a low binary inclination. Some fundamental parameters of the system are listed in Table 1.

The nature of the accretion-disc outflow in V603 Aql is not well determined. Previously, low-resolution (~6 Å) ultraviolet spectroscopy secured using the *International Ultraviolet Explorer* (*IUE*) satellite revealed a dominance of emission components in the

★ E-mail: rkp@star.ucl.ac.uk
† Hubble Fellow.
‡ Present address: Department of Physics, California State University, Fresno, 2345 E. San Ramon Ave, M/S MH37, Fresno, CA 93740-8031, USA.

resonance line profiles. The poor spectral resolution, however, generally makes it difficult to search for weak, blueshifted absorption components (see, e.g., Drechsel et al. 1981; Krautter et al. 1981; Selvelli & Cassatella 1981). More recently, Friedjung, Selvelli & Cassatella (1997) have described *HST* observations of V603 Aql taken with the Goddard High-Resolution Spectrograph (GHRS; G140M grating). The resonance line doublets of C IV, Si IV and N V were each covered in four 'subexposures' typically spanning 30 min (the different spectral lines were not, however, recorded simultaneously). They reported variable, but weak, blueward absorption in C IV and N V, but only emission in Si IV. The absorption extended to $\sim -2500\,\mathrm{km\,s^{-1}}$ and fluctuated over a time-scale of $\sim$10 min.

Using a more intensive *HST* GHRS data set, and simultaneous monitoring of key spectral lines, we demonstrate here that the outflow of V603 Aql produces highly episodic line absorption events (also seen in Si IV). We examine the velocity, optical depth and relative ionization behaviour of the absorption features, and search for empirical relations between the emission components of the resonance lines and the (also variable) continuum flux.

2 THE *HST* TIME-SERIES DATA SET

Our *HST* observations of V603 Aql were secured on 1996 October 6 UT, using the GHRS in accumulate (ACCUM) mode with the G140L grating in first order. The instrument set-up and data reduction procedures adopted were the same as previously described in our study of BZ Cam (PRWK). The analysis of V603 Aql is based on 90 'blue' subexposures (covering a wavelength range $\lambda\lambda$1140–1436) and 95 'red' subexposures ($\lambda\lambda$1367–1663), with a spectral resolution of 0.80 Å. Exposure times were 55.6 s for the 'red' spectra and 28.5 s for the 'blue' spectra, with a typical signal-to-noise ratio of $\sim$10 at λ1520 in individual subexposures. The observations spanned a total time of 5.06 h (i.e. about 1.5 orbital periods of V603 Aql). A summary of the main blocks of *HST* observations is given in Table 2, where we also label the principal 'time-bins' for the observations, which are referred to later in the paper. The relative orbital phases quoted are for $T_0(\mathrm{HJD} - 245\,0360.5) = 1.809\,797$ (i.e. the first spectrum in our data set).

Table 1. Fundamental parameters for V603 Aql.

Parameter	Value	Reference
Inclination, i	15°–20°	Warner (1976)
P_{orb}	0.138 154 d	Drechsel et al. (1982)
Distance	360 pc	Drechsel et al. (1981)
$E(B-V)$	0.05 ± 0.07	Gallagher & Holm (1974)
K velocity	$32\,\mathrm{km\,s^{-1}}$	Patterson et al. (1993)
$\dot{M}_{\mathrm{acc}}$	$5\times10^{-9}\,\mathrm{M_\odot\,yr^{-1}}$	Patterson (1984)

Table 2. Summary of *HST* observing blocks.

Time-bin	Time range (HJD − 245 0360.5)	No of spectra	Relative orbital phase
1	1.809 797–1.827 387	25	0.000–0.127
2	1.860 968–1.894 386	61	0.370–0.612
3	1.928 721–1.961 414	54	0.861–1.097
4	1.995 752–2.020 672	45	1.346–1.526

The mean of the blue and red subexposures is shown in Fig. 1. Aside from Lyα absorption (λ1216), the ultraviolet spectrum of V603 Aql is dominated by the resonance line doublets of Si IV $\lambda\lambda$1393.8, 1402.8 and C IV $\lambda\lambda$1548.2, 1550.8, plus features arising from C III λ1175.7 and He II λ1640.4. A variable N V $\lambda\lambda$1238.8, 1242.8 absorption profile is also present (though not obvious in the mean spectrum). We focus, in particular, on the characteristics of the outflow derived from the blueshifted absorption troughs of C III, N V, Si IV and C IV. The mean continuum flux level in Fig. 1 is comparable with that recorded in previous *IUE* studies of this system (see, e.g., references in Section 1).

3 ABSORPTION-LINE PROFILE VARIABILITY

A time-variable blueshifted absorption trough is unambiguously present in about 70 per cent of the C IV line profiles and about 40 per cent of the Si IV lines in our data set. The C IV absorption profile exhibits more extreme changes, with the equivalent width ranging between $\sim$0.5 and 5 Å, with the deepest troughs dropping to $\sim$60 per cent below the local continuum. We concentrate our study on the Si IV resonance line, however, since it is the most densely sampled line profile in our data set (i.e. common to, both, the 'red' and the 'blue' instrument settings), and has a wider doublet separation than C IV. Some examples of the line profile changes are shown in Fig. 2.

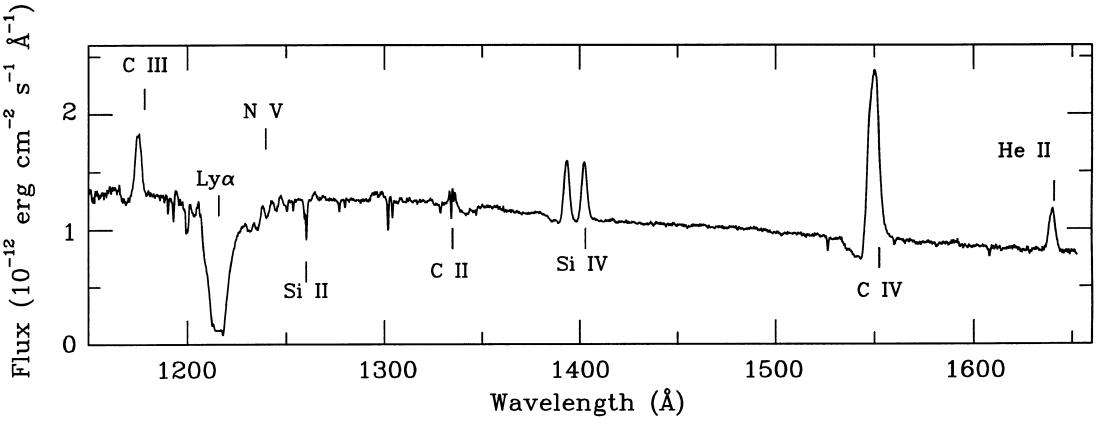

Figure 1. Mean of the blue and red *HST* GHRS subexposures of V603 Aql. Substantial and rapid blueward absorption line profile variability is present in time-series line profiles of C IIIλ1176, N V $\lambda\lambda$1240, Si IV $\lambda\lambda$1400 and C IV $\lambda\lambda$1550. The marked transitions of Si II and C II are interstellar. (No reddening corrections have been applied to the spectrum shown.)

The absorption is *always* seen at blueward velocities only, with a maximum extent of $\sim -2500\,\mathrm{km\,s^{-1}}$ in the resonance lines. (Note that the velocity scale in Fig. 2 is with respect to the blue components of the doublets.) On occasions, however, the blue wing of the absorption profile barely extends to ~ 500–$700\,\mathrm{km\,s^{-1}}$ (Fig. 2). In a qualitatively similar manner to BZ Cam (PRWK), the absorption troughs of V603 Aql are highly variable on very short time-scales; we highlight in Fig. 2, for example, simultaneous variations extending over $\sim 1500\,\mathrm{km\,s^{-1}}$ in just ~ 58 s. We attribute the variable blueward-extended absorption to the outflow from V603 Aql and not the disc. Disc absorption (symmetrical about zero velocity) is generally weak in this system. There are cases of individual subexposures where the blueshifted absorption is essentially absent, with no sign of 'underlying' absorption centred at rest velocity – even in N v, where 'filling-in' because of emission is not likely to be a substantial effect. The ultraviolet spectrum is also almost featureless between $\lambda\lambda$1420 and 1520, and between C IV and He II (Fig. 1).

In contrast to the absorption behaviour, the emission components of the resonance line doublets are relatively stable, and do not exhibit either corresponding or comparable fluctuations in strength or central velocity. The mean and standard deviation (s.d.) of the C IV and Si IV emission flux measured between 0 and $2000\,\mathrm{km\,s^{-1}}$ for redward doublet components (which therefore avoid complications arising from the transient blueward absorption features) is 3.53, s.d. 0.51 and 0.59, s.d. 0.16, respectively. (The units are in $10^{-12}\,\mathrm{erg\,cm^{-2}\,s^{-1}}$ for continuum-subtracted line profiles.) The mean central velocity of the He II λ1640 emission line – that is least affected in these ultraviolet spectra by absorption effects – is $\sim -84\,\mathrm{km\,s^{-1}}$ (s.d. $67\,\mathrm{km\,s^{-1}}$).

3.1 Episodic outflow events

The occurrence of blueshifted absorption in V603 Aql is highly episodic, with individual 'events' typically lasting less than $\sim$20 min ($\leqslant$10 per cent of the orbital period). To reveal details of the time evolution of the intermittent absorption, the individual Si IV line profiles are shown as grey-scale representations in Fig. 3, for the four principal time-bins labelled in Table 2. To emphasize the blueshifted absorption enhancements in this display, we have subtracted the mean Si IV profile from the individual profiles to 'remove' the relatively stable emission components.

Three absorption events are well recorded in our time series: (i) in time-bin 2 between $T(\mathrm{HJD} - 245\,0360.5) = 1.865$–$1.876$, (ii) in time-bin 3 between $T(\mathrm{HJD} - 245\,0360.5) = 1.933$–$1.942$, and (iii) in time-bin 4 between $T(\mathrm{HJD} - 245\,0360.5) = 1.997$–$2.005$. The average time-span for the formation and evolution of these episodes is $\sim$13.5 min, and the overall mean velocity range is ~ -500 to $-1250\,\mathrm{km\,s^{-1}}$. Irregular absorption features are also seen at other times (Fig. 3), but either their evolution is not well recorded in our data set, or they are extremely erratic. In addition, a fairly strong and abrupt event is noted between $T(\mathrm{HJD} - 245\,0360.5) = 2.013$ and 2.020, with a relatively steady velocity of $\sim -1750\,\mathrm{km\,s^{-1}}$. The velocity behaviour of the three principal events identified above is complex, and not monotonic as a function of time. In order to derive simple measures of the absorption enhancements seen, we analysed the residual Si IV features identified in Fig. 3 by (least-squares) fitting them with a Doppler absorption profile of the form

$$I = \exp\left\{-\tau_c \exp\left[-\left(\frac{v - v_c}{v_t}\right)^2\right]\right\} \qquad (1)$$

for both doublet components. For a given localized absorption feature (intensity I) the central velocity displacement (v_c) and width parameter (v_t) were constrained to be the same for both doublet components, and the central optical depths (τ_c) were held in the ratio $(\lambda_0 f)_1/(\lambda_0 f)_2$, where λ_0 and f are the rest wavelengths

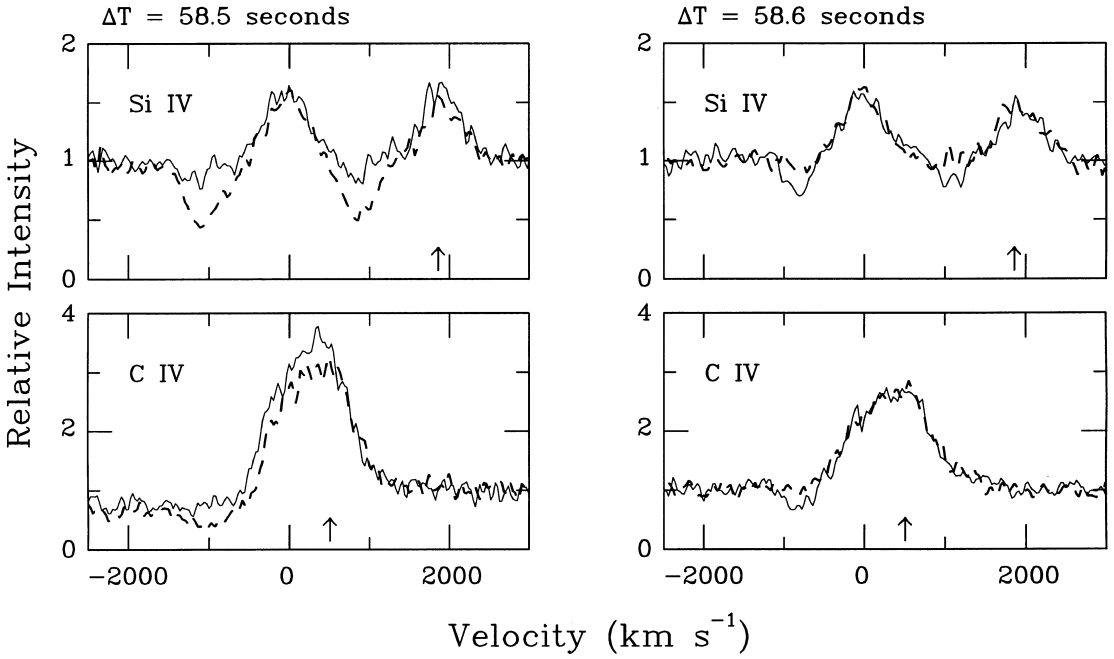

Figure 2. Examples of absorption variability on time-scales of $\sim$1 min, extending simultaneously over $\geqslant 1000\,\mathrm{km\,s^{-1}}$ in Si IV and C IV. (The left-hand panels show data set name z37v0208; subexposures 7 and 8, and the right-hand panels show data set name z37v020b; subexposures 11 and 12.) The velocity scale is with respect to the shortward components of the resonance line doublets, and the location of zero velocity for the red components is indicated by the vertical arrows. The line profile changes are almost entirely confined to blueward velocities.

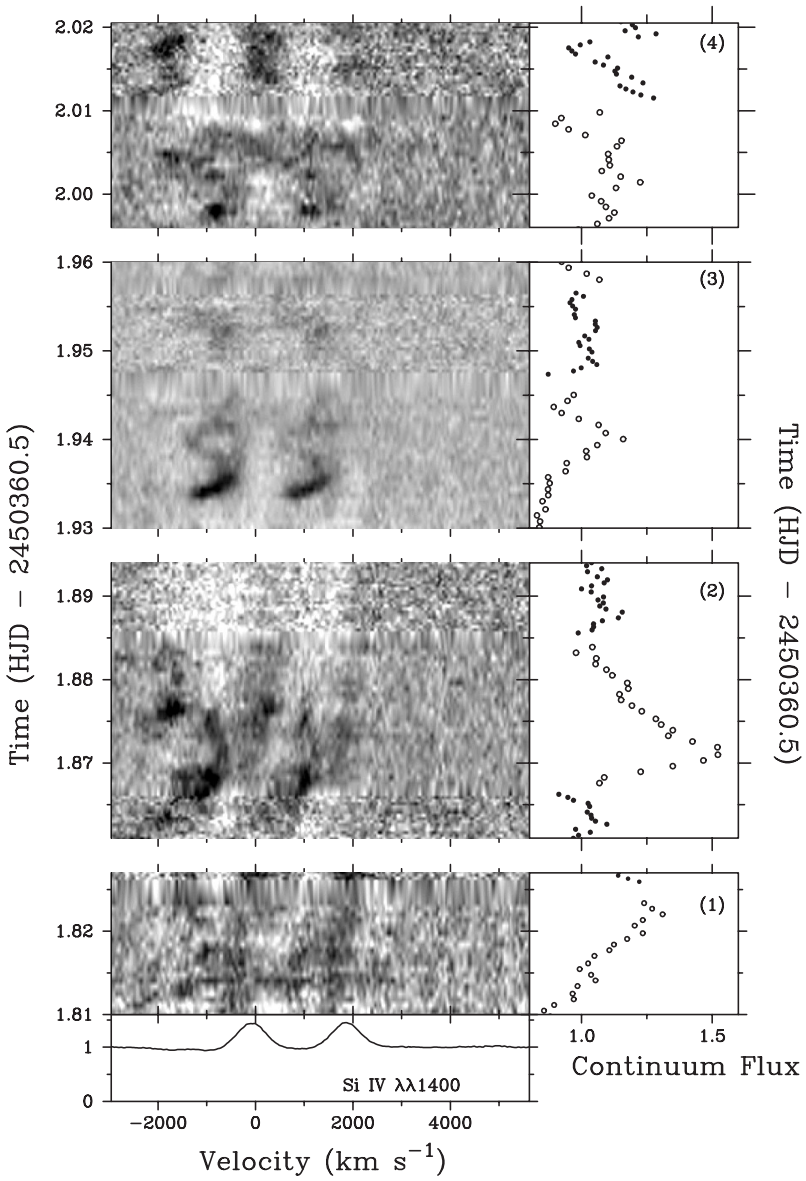

Figure 3. Grey-scale representations of variability in the Si IV λλ1400 lines of V603 Aql (see Section 3.1). The displays are darkest where the line optical depths are greatest. The line profile in the bottom panel is the mean of the subexposures (see Fig. 1), which has been subtracted from the individual subexposures for the purpose of these images. The mean continuum flux between λλ1415–1425 is shown in the panels on the right-hand side (see Section 4), where open circles are the red subexposures and filled circles are blue subexposures. The numbers in brackets represent the time-bins identified in Table 2. The units of continuum flux are 10^{-12} erg cm^{-2} s^{-1} Å^{-1}.

and the transition oscillator strengths, respectively, of the doublets. The parameters v_c, v_t and τ_c, were freely adjusted, and generally very good matches were obtained to the observed line profiles.

The central velocities and optical depths derived for the blueward Si IV doublet component are shown in Fig. 4 for the three main absorption episodes. There is no unique relation apparent between the optical depth and the central velocity of the different features, and the change in optical depth as a function of time is different in the three cases. In the episodes recorded in Fig. 4 (and Fig. 3) the *blueshifted* structure initially decelerates and then accelerates; it eventually decelerates again in the case of time-bin 3. Typically a deceleration or acceleration phase lasts only about 4 min, with linear rates between 1.1–2.7 and 1.1–3.6 km s^{-2}, respectively. The corresponding length-scales range between $\sim 5 \times 10^9$ to 2×10^{10} cm (i.e. approximately 5–20 white dwarf radii). The initial line-of-sight velocity dispersion of the absorption features increases, with typically a difference in the full-width at half-maximum of $\sim$150–250 km s^{-1} over the first 3–5 min. The widths are less reliably determined towards the end of the velocity progression of the features, since they become weaker in strength and 'break up' into multiple components. Overall, the mean full-width at half-maximum is $\sim$580 km s^{-1} (s.d. $\sim$215 km s^{-1}). There is no clear relation between the width of a given feature and its central Doppler velocity. In the case of the absorption event in time-bin 3, the width continues to increase from $\sim$350 km s^{-1} to $\sim$770 km s^{-1} during a period when the feature is decelerating and accelerating.

The episodic absorption variability in V603 Aql is present in other spectral lines, though they are not as intensely sampled in our data set as Si IV. We measured the total absorption equivalent

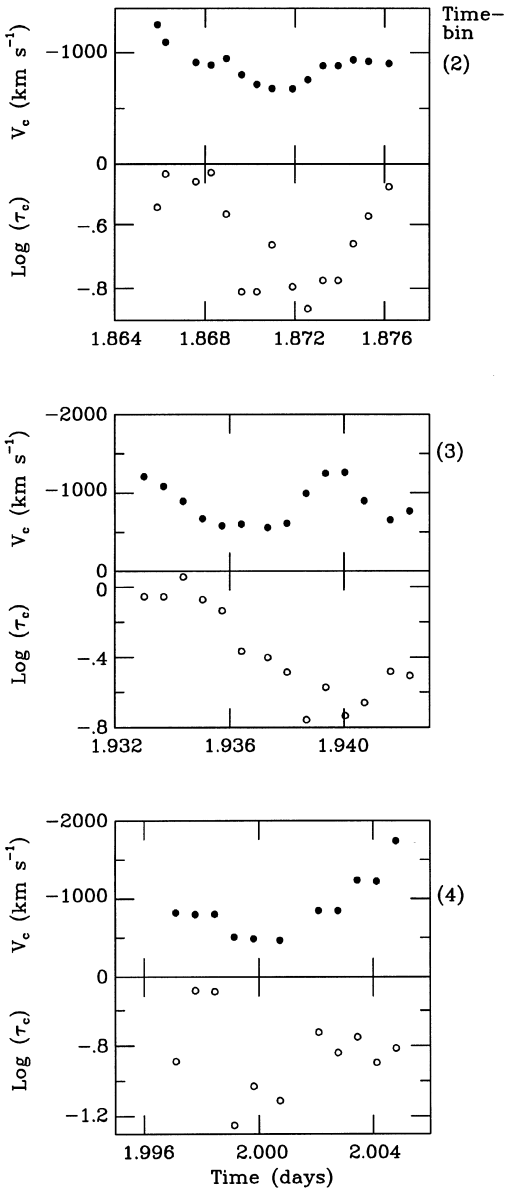

Figure 4. The central velocities (v_c) and optical depths (τ_c) of the three principal episodic absorption events observed in V603 Aql are shown for Si IV (blue doublet component) as a function of time. The time-bins labelled are defined in Table 2 (see also Fig. 3). Typical formal errors from the profile fits are ∼5 per cent for the velocities and ∼10 per cent for the optical depths.

width between −500 and −3000 km s^{-1} in normalized line profiles of C III λ1176, N V λ1240, Si IV λ1400 and C IV λ1550, for every *HST* subexposure in our time-series. The absorption behaviour between these lines is compared in Fig. 5. It is clear that absorption features of low and high ionization stages in V603 Aql vary in concert. The linear slopes in Fig. 5 are not the same, however, as the C III value is a factor of ∼2.5 lower than N V, and a factor ∼4.5 lower than C IV. In the optically thin regime, these results point to possible ionization structure in the absorbing gas. (Note, however, that the strongest absorption features are mostly present in our data during the red subexposures, and are thus generally not recorded in N V and C III.) Though the smaller doublet separation in C IV prevents reliable profile fitting of the form carried out in Fig. 4 for Si IV, it is clear that the episodic

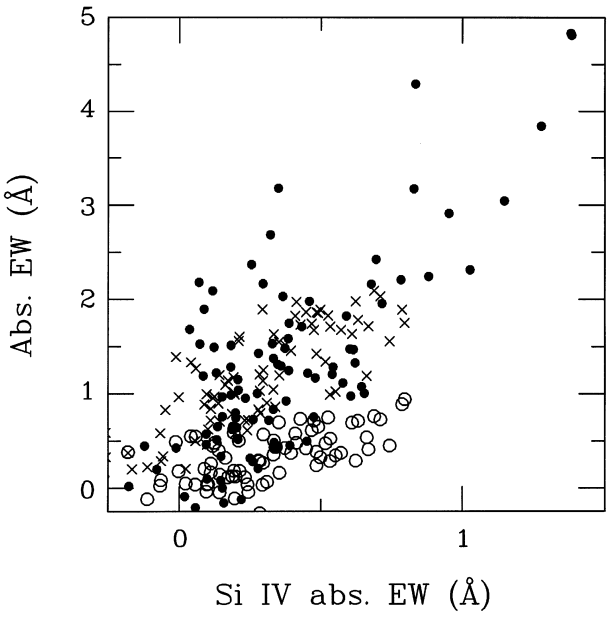

Figure 5. The absorption equivalent width in C III (open circles), C IV (filled circles), and N V (crosses) is compared to that in Si IV.

events are present at basically the same Doppler velocities in both ions. Furthermore, there is excellent agreement between the maximum absorption velocities observed simultaneously in the blue subexposures between C III, N V and Si IV, and between Si IV and C IV in the red subexposures. There is no evidence in these data for ionization-state-related velocity shifts in the absorption features.

The variability characteristics derived here point to the presence of stochastic and variable inhomogeneities in the outflow of V603 Aql. Their physical origin may relate, for example, to the action of instabilities in a radiatively driven accretion-disc wind [see, e.g., the model simulations of Proga, Stone & Drew (1998)]; we postpone further discussion to Section 5.

4 SHORT-TERM CONTINUUM FLUX CHANGES

There have been several previous reports, based on *IUE* spectroscopy, of a variable continuum flux in V603 Aql (e.g. Drechsel et al. 1981; Schwarzenberg-Czerny, Udalski & Monier 1992) corresponding to changes of ∼0.1 mag. Schwarzenberg-Czerny et al. (1992) claim a connection between the ultraviolet continuum radiation and the 63-min X-ray period (Udalski & Schwarzenberg-Czerny 1989) and suggest an origin of the fluctuations in a rotating, magnetic white dwarf. Note, however, that Arenas et al. (2000) find no evidence for periodic behaviour on this time-scale in their optical spectroscopic study.

The continuum fluxes in our *HST* subexposures are indeed variable with maximum fluctuations ∼40 per cent higher than the mean level (i.e. grossly above *HST* instrumentation effects). The mean continuum fluxes measured between λλ1415–1425 in the individual spectrograms are shown as a function of time in Fig. 3, where they are also compared with the incidence of episodic outflow events (Section 3). (Note, though we sampled the continuum overlap region between red and blue subexposures to maximize the data set, the measurements have an excellent correlation to flux changes apparent at other wavelengths in the

blue and red subexposures.) Two clear 'flares' are apparent during time-bins 1 and 2. In the latter case there is a steep rise (over ~4 min) and a slower 'decay' (over ~9 min). A weaker continuum 'flare' may also be present in the third time-bin. A Fourier analysis did not reveal an obvious short time-scale cycle for the flux changes; specifically the continuum variability shown in Fig. 3 is not modulated on the mooted 63-min X-ray period for this system.

The connection, if any, between the ultraviolet continuum flux variability and the episodic blueward absorption events is not well determined in these data. We note in Fig. 3, for example, that while the absorption features in time-bins 2 and 3 may be 'associated' with a temporary rise in the continuum level, this is not the case for time-bins 1 and 4. It is intriguing, however, that the overall time-scales involved in both variability phenomena are roughly the same. In the cases of time-bins 2 and 3 the peak in the continuum fluxes occur ~8–9 min after the initial detection of the localized absorption enhancements, though the potential 'lag' is not apparent at all in time-bin 1. The continuum flux changes are not correlated with the overall absorption strength or the strength of the line emission components.

5 CONCLUDING REMARKS

For brief periods of time the Si IV and C IV ultraviolet resonance lines in V603 Aql appear morphologically as 'classical' P Cygni profiles, i.e. with simultaneous blueward extended absorption and broad emission centred close to rest velocity. It is clear, however, from the variability characteristics presented here that the ultraviolet lines of the system derive their form from separate components, i.e. highly irregular and episodic absorption events that extend bluewards only, plus a considerably more stable emission source. The same is generally true for BZ Cam (PRWK) and may be the case for several high-luminosity, low-inclination, wind-driving CVs (see also V795 Her, Rosen et al. 1998). Certainly the notion of 'P Cygni' profiles presented in some previous low-resolution *IUE* studies of winds from CVs needs to be interpreted with caution based on results from high temporal and spectral resolution *HST* data. The relatively steady ultraviolet emission components may be associated with an extended thermal (non-scattering) wind emission source (e.g. Knigge & Drew 1997) with perhaps a modest rotational radial velocity signature. Alternatively, the emission may arise (at least partly) from a line-emitting hotspot on the disc (e.g. Knigge et al. 1994), in which case the absence of large orbital velocity variations in line-emission components of V603 Aql may simply reflect the low inclination of this system. The notion of a thermal emission source is also consistent with the fact that the net (continuum-subtracted) emission line flux is approximately constant and does not correlate with the continuum variations.

In V603 Aql, the safest – though not particularly well understood – indication of a disc outflow comes from the highly variable absorption events, that typically evolve over ~0.01 d. The sporadic events are *always* blueshifted, though the apparent velocity of a given feature can increase or decrease significantly over a very short time-scale. The time-dependent velocity and optical depth behaviour is different for sequential absorption episodes. The absorption features are erratic in terms of incidence, optical depth changes and velocity. In an admittedly short time-series *HST* GHRS data set, we find no evidence for cyclic or repeatable behaviour. A possible scenario is that the absorption arises from intermittent density enhancements in a highly structured and inhomogeneous disc-outflow with strong velocity perturbations. The origin of these rapidly evolving (~ a few minutes) inhomogeneities may relate to instabilities in a radiation-driven disc wind, that can potentially result in localized large-amplitude density and velocity structure (e.g. Proga et al. 1998). This scenario was previously applied in our empirical interpretation of the *HST* time-series data of BZ Cam (PRWK). In the case of V603 Aql, our rapid *HST* spectroscopy has provided considerably better defined cases of evolving localized absorption enhancements, where systematic variations in velocity, optical depth and acceleration could be examined.

The origin of the emission line source in V603 Aql is obviously a key issue (as is the case in other low-inclination wind-driving CVs). Since the ultraviolet absorption troughs in V603 Aql are so intermittent, our time-series data set provides some fine opportunities to examine the properties of apparently 'emission-only' line profiles. The maximum flux cases, i.e. exposures that are not 'contaminated' by blueward absorption, are compared in Fig. 6 between C III, Si IV, C IV and He II. The C IV emission line strength is substantially greater than the other ions, that was also generally true for the episodic absorption events (e.g. Fig. 5). There is no obvious or systematic difference between the velocity widths of lines of different ionization state, and the full-width at zero-intensity is ~1600 km s^{-1}. The peak intensities of the clearly resolved Si IV doublet components are almost identical, and certainly not in the 2:1 ratio expected in the simple optically thin case from the respective oscillator strength ratios. In the absence of irregular absorption components, these emission line profiles are very symmetric between the blueward and redward wings; any strong asymmetries here may have betrayed the presence of underlying absorption owing to a continuous 'smooth' outflow that has been 'filled-in' by the emission. The maximum extent of

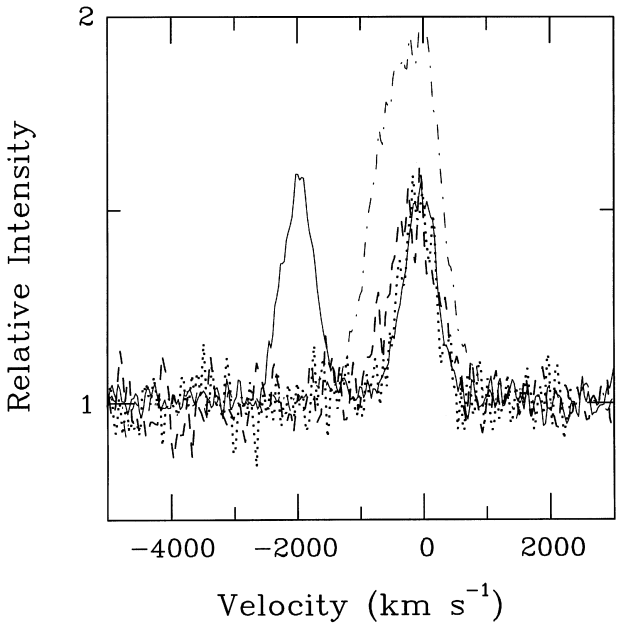

Figure 6. The emission profiles evident when the episodic absorption events are essentially absent are compared here for the cases of C III (dashed line), Si IV (solid line), C IV (dot-dashed line) and He II (dotted line). For the purpose of this figure, the peak intensity of the C IV line profile has been scaled down by 70 per cent. The velocity scale of the doublets is with respect to the red components.

the blue emission wing remains redward of $\sim -1000\,\mathrm{km\,s^{-1}}$, and therefore never overlaps the principal observed velocity domain of the episodic absorption events. The apparent absence of 'underlying' absorption (Fig. 6) does not, however, exclude the presence of a smooth disc wind in V603 Aql. In the kinematic models of rotating disc winds calculated by Shlosman & Vitello (1993), for example, if the disc inclination angle is smaller than the inner opening angle of the wind (i.e. less than $\sim 20°$), then we are essentially viewing an inner 'hole' in the biconical wind. In this case there is simply a dearth of absorbing gas. Alternatively, the smooth wind may just be too dilute to produce significant absorption in the ultraviolet ionization states monitored here.

We have provided new perspectives on the very short time-scale dynamics of the accretion-disc wind in V603 Aql, based on sensitive diagnostics offered by the ultraviolet resonance lines of luminous low-inclination CVs. A detailed physical interpretation of the outflow signatures cannot, however, be provided until we have an improved understanding of the overall absorption and emission line-formation mechanisms of this system.

ACKNOWLEDGMENTS

This work was based on observations with the NASA/ESA *Hubble Space Telescope*, obtained at the Space Telescope Science Institute, which is operated by the Association of Universities for Research in Astronomy, Inc. under NASA contract NAS 5-26555. Support for this work was provided by NASA through grant number GO-06661.01. Support for CK was provided by NASA through Hubble Fellowship grant HF-01109 awarded by the Space Telescope Science Institute. We are grateful for the resources provided by PPARC Starlink computer network in the UK. This work has used the Simbad data base, operated at CDS, Strasbourg, France. Some analysis was done with IRAF, which is distributed by the National Optical Astronomy Observatories, operated under cooperative agreement with the National Science Foundation. We also used STSDAS, which is distributed by the Space Telescope Science Institute.

REFERENCES

Arenas J., Catalán M. S., Augusteijn T., Retter A., 2000, MNRAS, 311, 135
Barnard E. E., 1919, ApJ, 49, 199
Clark D. H., Stephenson F. R., 1977, The Historical Supernovae. Pergamon Press, Oxford
Drechsel H., Rahe J., Holm A., Krautter J., 1981, A&A, 99, 166
Drechsel H., Rahe J., Wargau W., 1982, Mitt. Astron. Ges., 57, 301
Friedjung M., Selvelli P., Cassatella A., 1997, A&A, 318, 204
Gallagher J. S., Holm A. V., 1974, ApJ, 189, L123
Haefner R., Metz K., 1985, A&A, 145, 311
Knigge C., Drew J. E., 1997, ApJ, 486, 445
Knigge C., Drew J. E., Hoare M., la Dous C., 1994, MNRAS, 269, 891
Krautter J., Klare G., Wolf B., Duerbeck H. W., Rahe J., Vogt N., Wargau W., 1981, A&A, 102, 337
Patterson J., 1984, ApJS, 54, 443
Patterson J., Thomas G., Skillman D. R., Diaz M., 1993, ApJS, 86, 235
Payne-Gaposchkin C., 1957, The Galactic Novae. North-Holland, Amsterdam
Prinja R. K., Ringwald F. A., Wade R. A., Knigge C., 2000, MNRAS, 312, 316 (PRWK)
Proga D., Stone J. M., Drew J. E., 1998, MNRAS, 295, 595
Rosen S. R., Prinja R. K., Drew J. E., Mason K. O., Howell S. B., 1998, MNRAS, 299, 305
Schwarzenberg-Czerny A., Udalski A., Monier R., 1992, ApJ, 401, L19
Selvelli P. L., Cassatella A., 1981, in Chiosi C., Stalio R., eds, 59th Trieste Colloq, Effects of Mass Loss on Stellar Evolution. Reidel, Dordrecht, p. 515
Shlosman I., Vitello P., 1993, ApJ, 409, 372
Udalski A., Schwarzenberg-Czerny A., 1989, Acta Astron., 39, 125
Warner B., 1976, in Eggleton P., Mitton S., Whelan J., eds, Proc. IAU Symp. 73, Structure and Evolution of Close Binary Systems. Reidel, Dordrecht, p. 85
Weaver H., 1974, in Contopolous G., eds, Highlights of Astronomy, Vol. 3. Reidel, Dordrecht, p. 423

This paper has been typeset from a TEX/LATEX file prepared by the author.